Chapter 57
Experimental Verification and Improvement of Dynamic Characterization Method for Structural Joints

Şerife Tol and H. Nevzat Özgüven

Abstract Mechanical connections play a significant role in predicting the dynamic characteristics of assembled structures accurately. Therefore, several methods were developed to determine equivalent dynamic models for joints. In this paper an experimental identification method based on FRF decoupling and optimization algorithm is proposed for modeling structural joints. The method developed is an extension of the method proposed by the authors in an earlier work. In the method proposed in our earlier work FRFs of two substructures connected with a bolted joint are measured, while the FRFs of the substructures are obtained analytically or experimentally. Then the joint properties are calculated in terms of translational, rotational and cross-coupling stiffness and damping values by using FRF decoupling. In this present work, an optimization algorithm is used to update the values obtained from FRF decoupling. The validity and application of the proposed method are demonstrated with experimental case studies. Furthermore, the effects of bolt size on joint dynamics are also studied by making a series of experiments and identifying the joint parameters for each case.

Keywords Structural joints • Joint modeling • FRF decoupling • Experimental identification • FRF measurement

57.1   Introduction

Many engineering structures are assembled from components by using a variety of connections; such as bolted, riveted, welded and bonded joints. Due to the effect of joints on the dynamic behavior of assembled structures, the importance of joint modeling or the identification of joint dynamic properties has become more and more significant. Reliable dynamic models for structural systems are based on the accurate identification of joint parameters. Since dynamic modeling of joints analytically is very difficult and usually not so accurate, experimental methods are used as an alternative for establishing a mathematical model for a joint.

Experimental methods can be classified as modal based methods and frequency response function (FRF) based methods. In the former class of methods, modal parameters identified from modal testing are utilized in modeling of joints. However, for structures including closely spaced modes or with large modal damping, accurate modal parameters cannot be easily obtained. Moreover, due to the nature of the modal parameter extraction process, results inevitably contain errors to some degree. In order to overcome this shortcoming, FRF based methods have been proposed in the literature.

The basic strategy in most of the FRF based joint identification methods is to use FRFs of individual substructures without joints and also those of the assembled system (structure with joints) to obtain information about the joint properties [1]. In the past decade, there were several researchers who focused on the identification of joint properties using FRF based methods. However, due to the inherent noise in measurements and different sensitivities of the formulations to noise, accuracy of the identification results differs. The reasons for this sensitivity and ways of coping with them are investigated in several studies

Ş. Tol
Department of Mechanical Engineering, Middle East Technical University, Ankara 06800, Turkey

George W. Woodruff School of Mechanical Engineering Georgia Institute of Technology, 801 Ferst Drive Atlanta, GA 30332-0405, USA
e-mail: stol3@gatech.edu

H.N. Özgüven (✉)
Department of Mechanical Engineering, Middle East Technical University, Ankara 06800, Turkey
e-mail: ozguven@metu.edu.tr

[2–10]. For example, Tsai and Chou utilized the substructure FRF synthesis method in the formulation of the joint parameter identification [2]. Wang and Liou [3] improved the work of Tsai and Chou [2]. They avoided inversion of matrices in their algorithm; hence, tried to reduce noise effect in the identification. Hwang [4] used the same formulation and improved the results using an averaging process to exclude highly sensitive regions. Ren and Beards [6] developed a generalized coupling method taking into account the physical restrictions of the real structures, and identified joint parameters with this new method. However, they avoided stiff joints in order to avoid ill-conditioned matrices, and used weighting techniques for better accuracy [1]. Celic and Boltezar [7] improved the method developed by Ren and Beards [1,6] by including the effects of rotational degrees of freedom (RDOFs). Another approach similar to the one presented in [6] is proposed by Maia et al. [8]. They reformulated the impedance uncoupling technique, and identified joints without using joint related FRFs. However, this method has not been validated with an experimental study. Yang et al. [9] derived identification equations employing substructure synthesis. They modeled a joint in terms of translational and rotational stiffness values and used singular value decomposition to avoid noise effect. However, joint damping was not included in their work.

In this study an experimental identification method based on FRF decoupling and optimization algorithm is proposed for modeling structural joints. The method developed is an extension of the method proposed by the authors in an earlier work [11]. In the method proposed in the earlier work FRFs of two substructures connected with a bolted joint are measured, while the FRFs of the substructures are obtained theoretically or experimentally. Then the joint properties are calculated in terms of translational, rotational and cross-coupling stiffness and damping values by using FRF decoupling. In this present work, an optimization algorithm is proposed to update the values obtained from FRF decoupling. The validity and application of the proposed method are demonstrated with several experimental studies by using beams connected with hexagonal bolts.

57.2 Theoretical Formulation

57.2.1 Identification of Dynamic Properties of Joints Using FRF Decoupling

Frequency response function coupling is one of the most widely used methods in the literature in analyzing two structures coupled elastically. Consider substructures A, B and their assembly (structure C) obtained by coupling them with a flexible element as shown in Fig. 57.1. The coordinates j and k represent joint degrees of freedoms (DOFs), while r and s are the ones that belong to the selected points of substructures A and B, respectively, excluding joint DOFs.

By using the elastic coupling equations (explained in more detail in [11]), it is possible to decouple and thus to calculate the complex stiffness matrix representing joint stiffness and damping as shown below:

$$[K*] = [[H_{jr}].[[H_{rr}] - [H_{rr}^C]]^{-1}.[H_{rj}] - [H_{jj}] - [H_{kk}]]^{-1} \qquad (57.1a)$$

$$[K*] = [[H_{ks}].[H_{rs}^C]^{-1}.[H_{rj}] - [H_{jj}] - [H_{kk}]]^{-1} \qquad (57.1b)$$

$$[K*] = [[H_{jr}].[H_{sr}^C]^{-1}.[H_{sk}] - [H_{jj}] - [H_{kk}]]^{-1} \qquad (57.1c)$$

$$[K*] = [[H_{ks}].[[H_{ss}] - [H_{ss}^C]]^{-1}.[H_{sk}] - [H_{jj}] - [H_{kk}]]^{-1} \qquad (57.1d)$$

As it was discussed in the earlier work of the authors [11] the most accurate results are obtained with Eq. (57.1a). However, from the experimental applicability point of view among the decoupling equations the most practical one is Eq. (57.1d). Equation (57.1a) requires the measurements of FRFs which belong to substructure A at both joint and non-joint DOFs, which
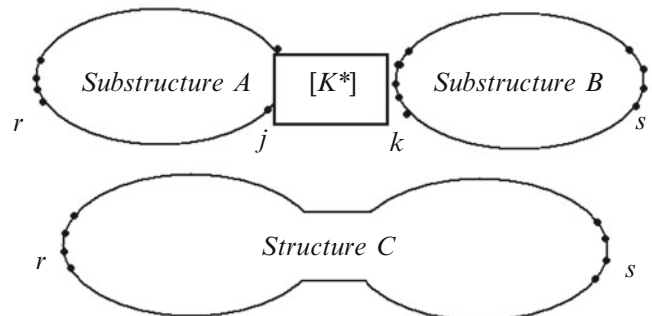
Fig. 57.1 Elastic coupling of two substructures

Fig. 57.2 Coupled structure with
a bolted joint
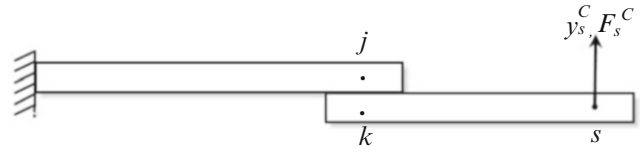
is very time consuming and expensive. Furthermore, when Eq. (57.1a) is used it is not possible to obtain cross-coupling FRFs including rotational DOF (RDOF) information between joint and non-joint coordinates. On the other hand, when Eq. (57.1d) is used, only the translational and rotational FRFs at the joint coordinate of the substructure A are required to be measured, since FRFs of the substructure B can be obtained theoretically. Hence, it can be concluded that the most practical decoupling equation is the last one (Eq. (57.1d)). Therefore, being different from our previous study, Eq. (57.1d) is employed in the present study.

Furthermore, in the present study, in order to overcome the difficulties in measuring RDOF related FRFs of the coupled structure in experiments, only translational DOF (TDOF) related ones are measured and used in the identification equation. In this approach only one translational FRF at the tip point (points) of the coupled structure (see Fig. 57.2) is used in the decoupling equation. Hence, in the identification process, the need for the estimation of RDOF related FRFs belonging to the coupled structure is eliminated while keeping joint model unchanged with translational, rotational and cross-coupling elements. It is also observed in the experimental studies that, if the number of TDOF related FRFs is increased, the identification results get better.

Then, the matrix dimensions will be as follows:

$$[K*] = [[H_{ks}].[[H_{ss}] - [H_{ss}^C]]^{-1}.[H_{sk}] - [H_{jj}] - [H_{kk}]]^{-1}$$
$$(2x2)(2x1)(1x1)(1x1)(1x2)(2x2)(2x2) \qquad\qquad (57.2)$$

After calculating the complex joint stiffness matrix, the stiffness and damping values representing the joint dynamics are obtained from the real and imaginary parts of the matrix elements, respectively.

57.2.2 Estimation of FRFs for RDOF and Unmeasured Coordinates

Analytically, all elements of an FRF matrix can be calculated easily. However, in real life applications, measuring all the elements of an FRF matrix experimentally, when there are many points under consideration, is very time consuming and expensive; furthermore, it may not be possible in every case due to several different reasons. In the method proposed we need the full receptance matrix for the DOFs we are interested in. In order to obtain complete FRF matrix the structure should be excited from all points we are interested in. However, in testing usually only one column of the FRF matrix is obtained by exciting the structure from a single point and measuring responses at all other points we are interested in. Therefore, we will usually have incomplete data as far as the experimentally measured FRF matrices are considered. In this work, the missing FRF data is obtained by using FRF synthesis after extracting modal parameters by modal testing.

Another difficulty in obtaining experimentally measured FRF matrices is the measurement of RDOF related FRFs which are required in the identification equations. However, the measurement of FRFs related to RDOFs is very difficult and requires special equipment. Therefore, in this study the RDOF related FRFs are estimated by using a procedure based on the well known finite difference formulation proposed by Duarte and Ewins [12]. After measuring three translational FRFs, the RDOF related FRF can be obtained easily.

57.2.3 Optimization and Joint Parameter Updating

In this study it is intended to obtain constant joint parameters representing the joint stiffness and joint damping in the whole frequency band of interest, assuming that bolted joints introduce frequency independent stiffness and damping. In our previous study, stiffness and damping values are identified at every frequency in the mode which is sensitive to the joint dynamics by using Eq. (57.1a) and then the average of these identified values is taken as the resultant value [11]. However, in real life applications due to the measurement errors at each level and numerical errors associated with matrix inversion,

the variation of identified values with frequency may be considerable and it may not be easy to decide on the best frequency range to be used even in the mode which is sensitive to joint dynamics for identifying the joint properties correctly. Young et al. proposed a solution for this problem by taking some fit values from the identification curve and using these values to redefine the joint stiffness matrix in a dynamic manner [13]. However, they do not obtain present enhanced results in their work.

In this present study, an optimization algorithm is developed using "fminunc" command of MATLAB to optimize the joint properties such that regenerated and measured FRFs for the bolted assembly match at all the modes in the frequency region of interest. Using the identified joint parameters from Eq. (57.1d) as initial estimates, this algorithm updates the joint parameters by minimizing the sum of the difference between the squares of the actual and regenerated receptance amplitudes calculated at each frequency. The key point for the success of the optimization process lies in starting with a good initial estimate. In fact, one can obtain a set of joint parameters starting with some arbitrary initial estimates and identify joint parameters which may yield the correct FRF curve used in the optimization process. However, when these values are used in a new assembly, the resulting FRFs will not be correct, due to the lacking of a physical basis of the joint dynamic properties. Hence, in order to have a correct dynamic modeling of the joint, it is concluded that, initial estimates used in optimization process for the joint parameters should be close to the actual values, which can be obtained by using the identification method summarized in Sect. 57.2.2 above. The application of the proposed updating method combined with the identification method developed in our previous study [11] is illustrated and the methods are verified with several experiments conducted by using beams connected with hexagonal bolts.

57.3 Experimental Studies

In this section three experimental studies are given to verify the method suggested and illustrate the accuracy and applicability of the method in real life applications. In these experiments, the joints obtained connecting two steel beams with M10 × 35, M8 × 35 and M6 × 30 bolts are identified and the models obtained for the connections are used in predicting FRFs either at the points which are not used in identification, or for new assemblies. In all experiments, a cantilever steel beam is used as substructure A, and it is connected to a free-free steel beam (substructure B) with the same cross section.

In the first experimental study, the joint obtained connecting two beams with M10 × 35 bolt is identified and the joint model is used to predict the FRFs of another point on the assembled system which is not used in identification computations. The predicted FRFs are compared with experimentally measured ones. In the second experimental study, a similar joint with M8 × 35 bolt is identified and the dynamic model of the joint is used to predict FRFs of a different coupled structure obtained with the same bolt but with a longer steel beam. The predicted FRFs are again compared with experimentally measured ones. Finally, in the last experimental study, a similar joint with M6 × 35 bolt is identified and the dynamic model of the joint is used to predict FRFs of the same beams connected with two M6 × 35 bolts. The predicted FRFs are once again compared with experimentally measured ones.

In the experiments, LMS modal test system, PCB impact hammer, PCB miniature sensors are used. Frequency resolution is selected as 0.25 Hz and the frequency range is set to 512 Hz using soft tip of the impact hammer. For the free-free tests of the substructure B, the frequency range is set to 1,024 Hz using hard tip of the impact hammer. A sufficient pre-trigger level is selected and during the experiments it is assured that all pulses are captured.

57.3.1 Experimental Study I: Beams Connected with M10 × 35 Hexagonal Bolt

In this case study A2-70 M10 × 35 hexagon head bolt is used and the tightening torque is set to 30 Nm. The test set-up used is shown in Fig. 57.3. The dimensions of two stainless steel beams are as follows: Length of substructure A, $L_A = 0.3$ m; length of substructure B, $L_B = 0.335$ m; width of the beams: 0.015 m, height of the beams: 0.010 m.

In the experimental identification of the bolted joint, FRFs of substructure A which has fixed-free boundary conditions are measured; while the FRFs of substructure B which has free-free boundary conditions are obtained theoretically by using FE modeling and also employing the measured modal and structural parameters of the beam. In the testing of the substructure B, it is suspended with elastic cords. After exciting the substructure B from the tip point, the tip point FRFs are experimentally obtained as shown in Fig. 57.4 and the modal parameters are identified. From the tests performed on substructure B, the following parameters are obtained: elastic modulus $E = 1.9210^1$N/m^2; density $\rho = 7,604$ kg/m^2, damping ratio for the first elastic mode $= 0.0005$. Then, these values are used in the FE model of the free-free beam in calculating the required FRFs of the substructure B ($[H_{kk}]$, $[H_{ks}]$, $[H_{sk}]$ and $[H_{ss}]$), accurately.

Fig. 57.3 Single bolt connection
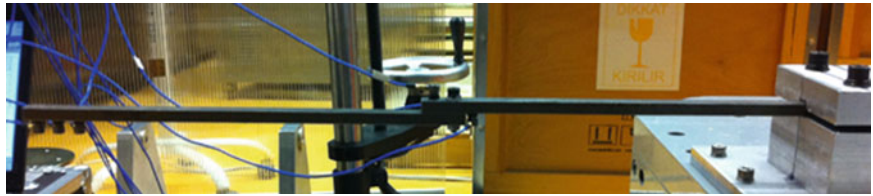
Fig. 57.4 (**a**) Testing of substructure B, (**b**) measured and theoretical (after tuning) FRFs at the tip point
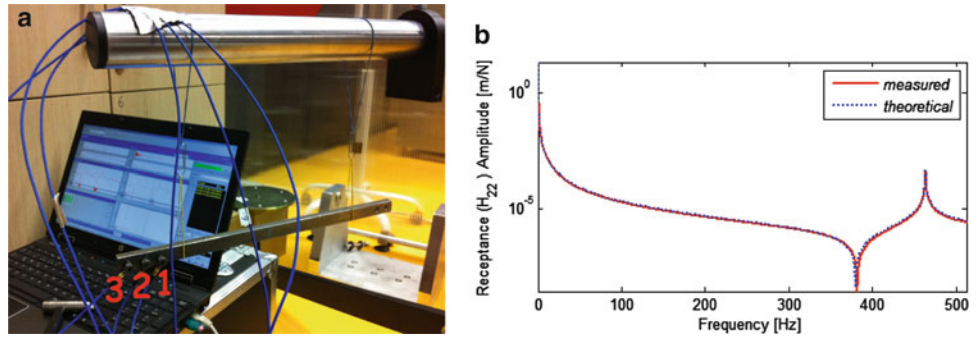
Fig. 57.5 Close accelerometers method for substructure A
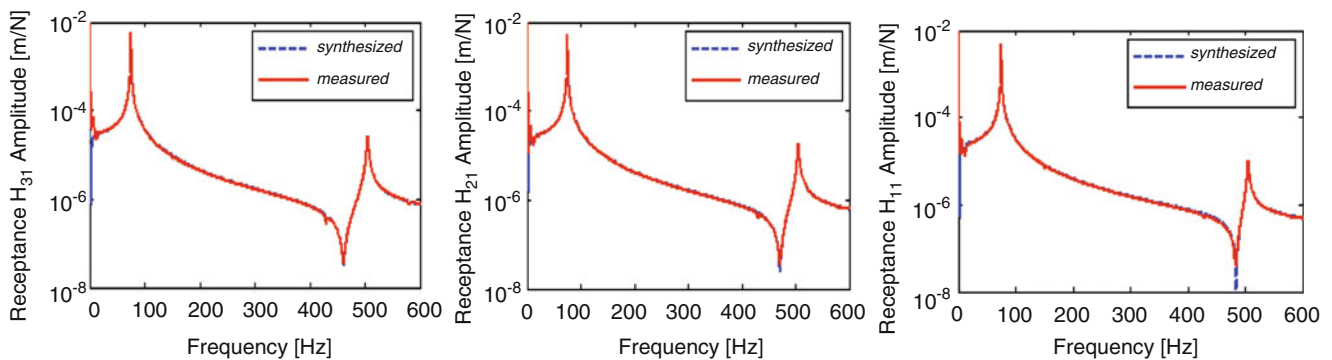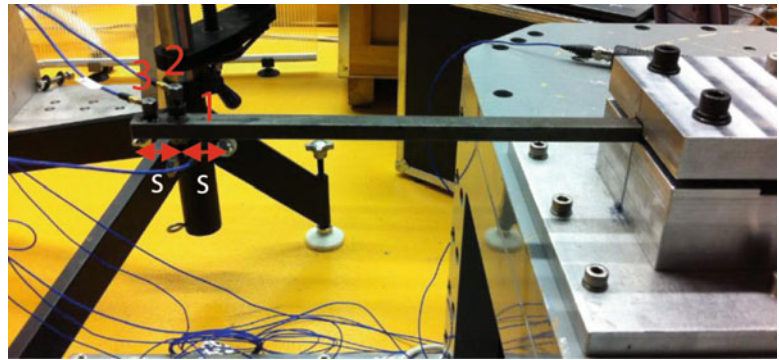
Fig. 57.6 FRF synthesis for substructure A

In order to estimate the RDOF related FRFs of substructure A, three accelerometer measurements are taken by exciting the system at point 1. The accelerometers are located with spacing, s, of 0.015 m as shown in Fig. 57.5. After completing the FRF measurements, system identification is performed using the LMS modal analysis software, and required parameters for the FRF synthesis are obtained in terms of upper and lower residuals, modal vectors, natural frequencies and damping ratios. Then, translational FRFs at the tip point of substructure A are obtained as shown in Fig. 57.6.

After obtaining the translational FRFs at the tip point, using the second order finite difference formula, rotational FRFs are estimated at point 2 as shown in Fig. 57.7.

Fig. 57.7 Rotational FRF
estimation for substructure A
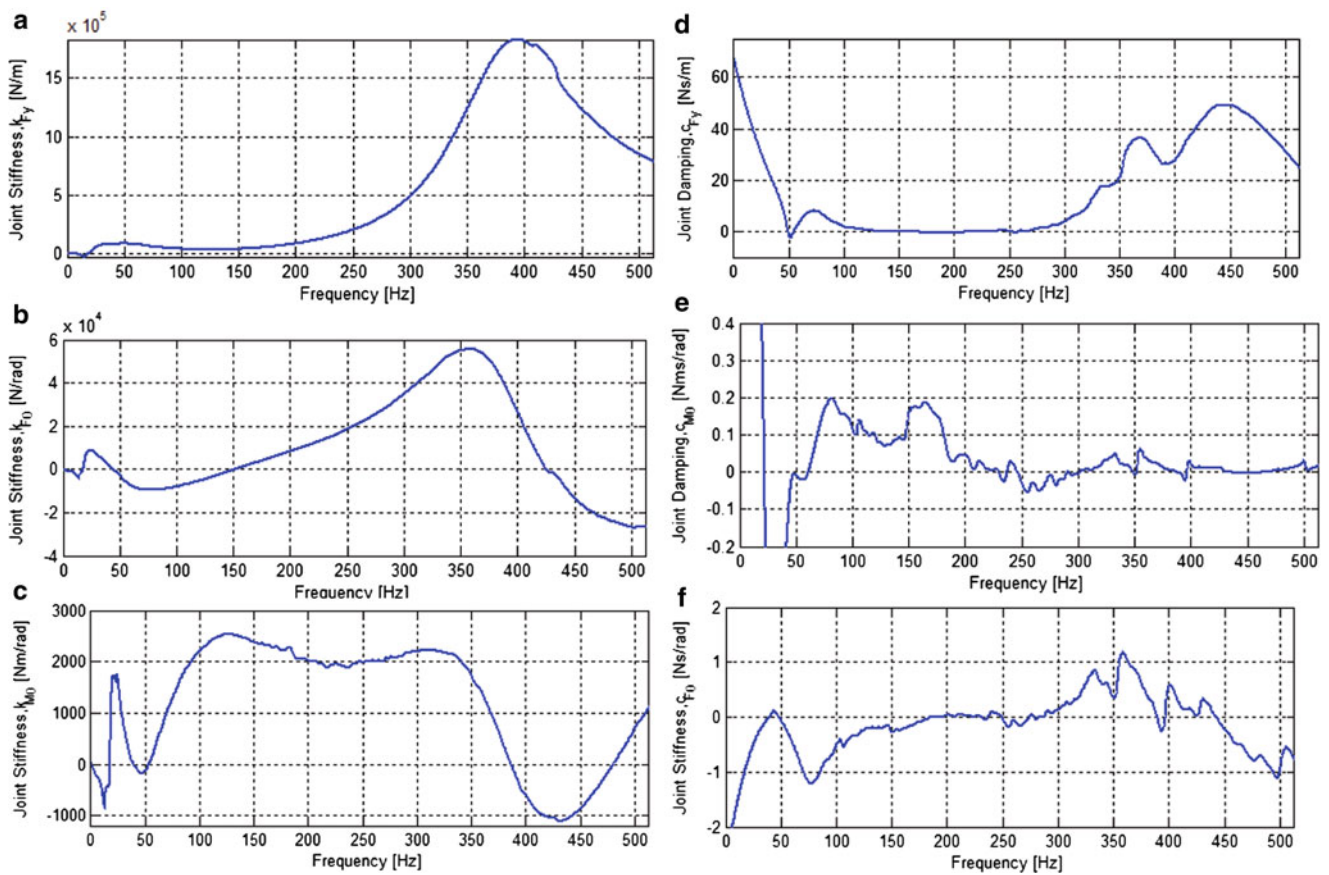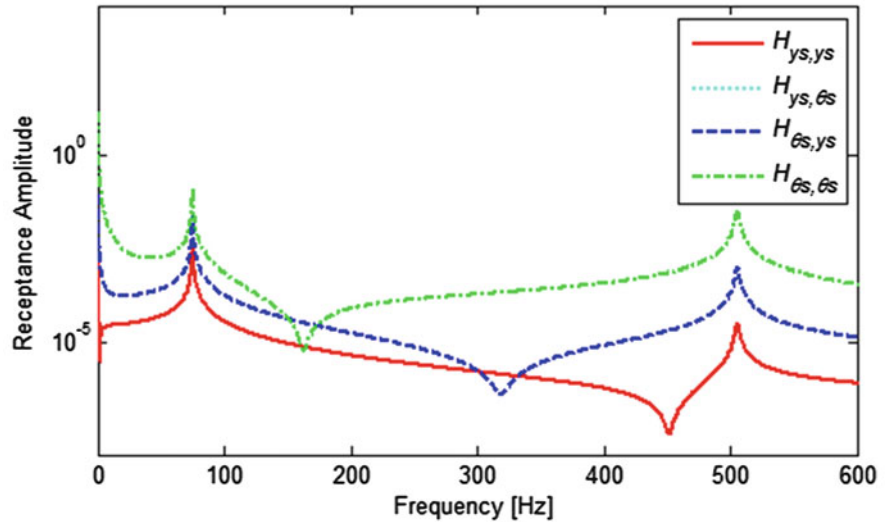
Fig. 57.8 Identification of joint stiffness and joint damping (**a**) translational joint stiffness, (**b**) cross-coupling joint stiffness, (**c**) rotational joint stiffness, (**d**) translational joint damping, (**e**) cross-coupling joint damping, (**f**) rotational joint damping

In this case study the properties of the bolted joint are extracted with the simplified identification approach, in which only one of the translational direct point FRF measured at the tip point 2 of the structure is used. The identified joint stiffness and damping values are shown in Fig. 57.8. It is seen that the joint properties are changing with frequency and the best frequency range to determine the joint properties are not obvious. When the identification results at some modes of the coupled structure are used in the coupling equations, regenerated FRFs of the coupled structure are found to be exactly the
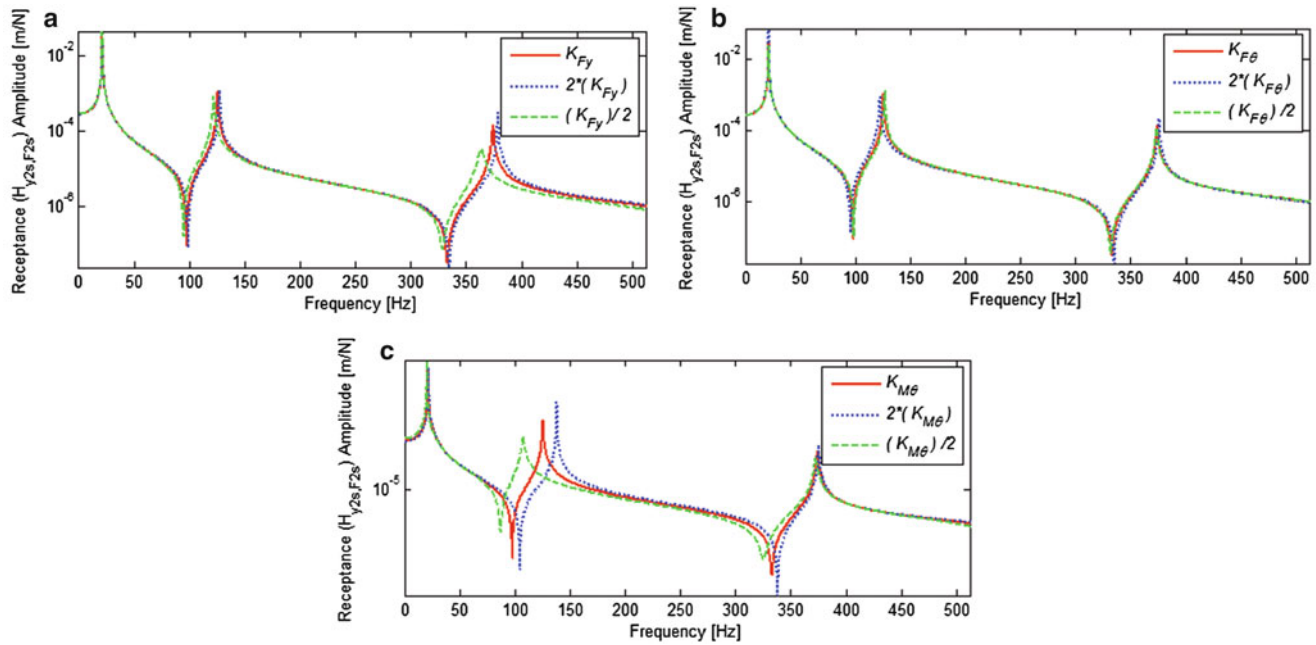
Fig. 57.9 Sensitivity of the receptance of the coupled structure to (**a**) translational joint stiffness, (**b**) cross-coupling joint stiffness, (**c**) rotational joint stiffness

Table 57.1 Joint parameters of the M10 × 35 bolted connection

	k_{Fy} (N/m)	$k_{F\theta}$ (N/rad)	$k_{M\theta}$ (N.m/rad)	c_{Fy} (N.s/m)	$c_{F\theta}$(N.s/rad)	$c_{M\theta}$ (N.m.s/rad)
Initial estimates	$1.71*10^6$	$5.12*10^4$	$2.5*10^3$	34.72	0.646	0.073
Updated	$2.02*10^6$	$2.47*10^4$	$2.8*10^3$	34.41	0.635	0.077

same with the measured FRFs at these modes, but showing differences at other modes, indicating that these values cannot represent the bolted joint accurately at every mode. Yet, it was suggested in the previous work of the authors [11] to use the values identified at the frequencies where FRFs are sensitive to joint dynamics, and take the average of them for the best possible identification. Therefore, first the sensitivity analysis given in Fig. 57.9 is performed before making identification.

From the sensitivity analysis, it is seen that, translational and cross-coupling joint stiffness is effective at the third mode, while rotational stiffness is effective at both second and third modes. Therefore, the values of translational and cross-coupling joint stiffness and damping identified at the third mode and rotational parameters identified at the second mode give the best possible values. Then, these values are used as initial estimates and updated with the algorithm mentioned above. Starting with initial estimates from the identified results at the second mode for rotational parameters, the third mode for translational and cross-coupling parameters, the updated joint parameters are obtained as given in Table 57.1.

By using the updated joint parameters, receptances of the assembled system are regenerated and they are compared with the measured receptances in Fig. 57.10. It can be seen from the comparison that the receptances regenerated by using the updated joint parameters perfectly match with the measured FRFs. It is interesting to note that while some joint parameters do not change much after updating, especially some cross terms change significantly, but the overall effect of updating is very significant at some modes as can be seen from Fig. 57.10.

Finally, by using the updated joint parameters, the FRFs of the coupled structure at points 1 and 3 (see Fig. 57.5), which are not used in the identification of joint properties, are obtained. It can be seen from Fig. 57.11 that the receptances calculated by using the updated joint parameters perfectly match with the measured FRFs. Hence, it can be concluded that, the joint properties are identified accurately.

57.3.2 *Experimental Study II: Beams Connected with* **M8 × 35 Hexagonal Bolt**

In this experimental study, the properties of a joint with M8 × 35 mm hexagon head bolt are determined. In the identification of the bolted joint parameters, only one of the translational FRF measured at the tip point (point 2) of the coupled structure is

Fig. 57.10 Regenerated FRF, $H_{y2s.F2s}$, of the coupled structure using updated joint properties
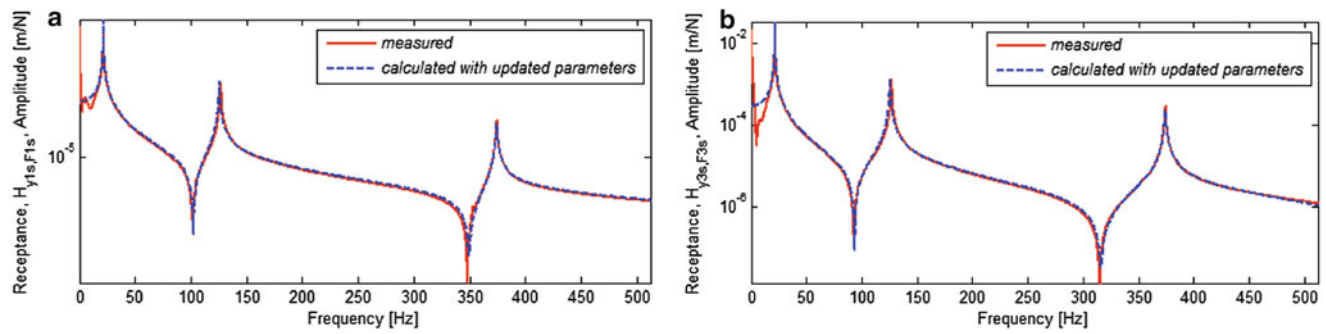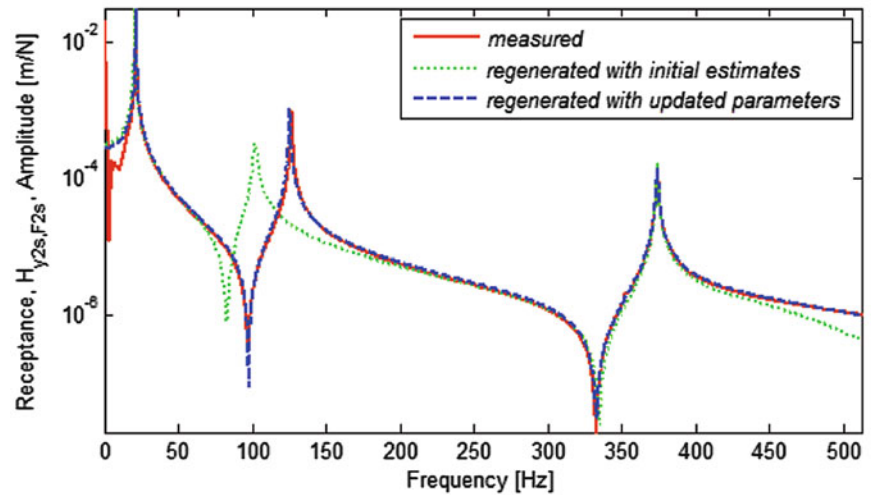
Fig. 57.11 Calculated FRFs of the coupled structure using updated joint properties (**a**) $H_{y1s.F1s}$, (**b**) $H_{y3s.F3s}$

Table 57.2 Joint parameters of the M8 × 35 bolted connection

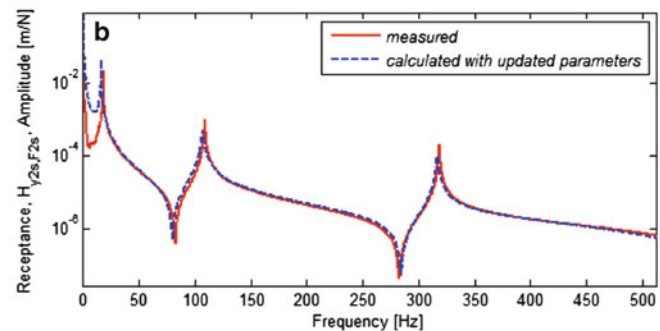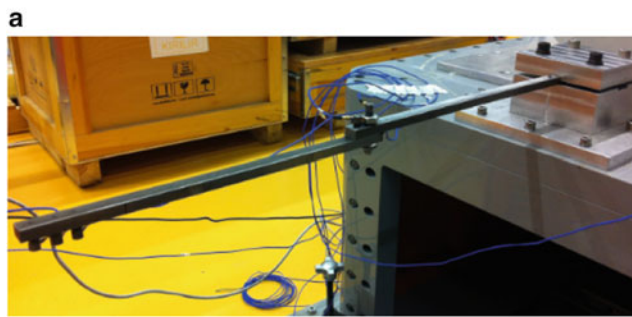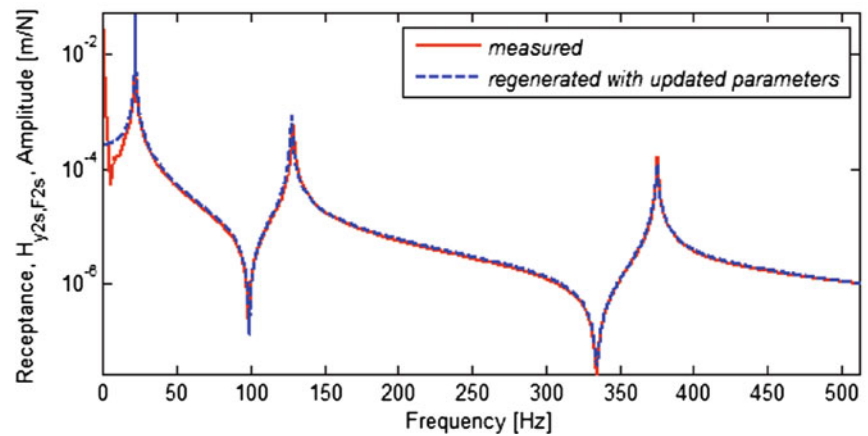|	k_{Fy} (N/m)	$k_{F\theta}$ (N/rad)	$k_{M\theta}$ (N.m/rad)	c_{Fy} (N.s/m)	$c_{F\theta}$ (N.s/rad)	$c_{M\theta}$ (N.m.s/rad)
Initial estimates	$1.83*10^6$	$5.53*10^4$	$2.9*10^3$	42.2	0.848	0.139
Updated	$2.14*10^6$	$2.66*10^4$	$3.2*10^3$	41.2	0.845	0.119

used. Afterwards, the identified joint parameters are employedto calculate theoretically the FRFs of a different coupled structure constructedwith steel beams having the same material and cross sectional dimensions, and the same bolt but different length. Then, the estimated FRFs are compared with the measured ones.

Firstly, again starting with initial estimates from the identified results at the second mode for rotational parameters, at the third mode for translational and cross-coupling parameters, the updated joint parameters are obtained as given in Table 57.2. The initially identified values are also shown in the same table. By using the updated joint parameters, receptances of the assembled system are regenerated and they are compared with the measured receptances in Fig. 57.12. It can be seen from the comparison that the receptances regenerated by using the updated joint parameters perfectly match with the measured FRFs.

After obtaining the joint parameters of the connection with M8 bolt, a different verification study is performed. In this verification study, a new substructure A with a length of 0.35 m (longer than the previous one) is used as shown in Fig. 57.13. By using the measured FRFs of the new substructure A, but joint parameters identified from the previous system (with a shorter substructure A), receptance of the new assembled system at the tip point is calculated, and it is compared with the measured receptance in Fig. 57.13. It can be seen from the comparison that the receptances predicted by using the joint parameters identified from a different assembly perfectly match with the measured FRFs of another assembly. Then it can be concluded that, once the joint properties are identified, it can be used for another structure having the same connection (the same material and cross sectional dimensions for the beams and the same bolt).

Fig. 57.12 Regenerated FRF, $H_{y2s.F2s}$, of the coupled structure using updated joint properties

Fig. 57.13 (**a**) New assembly with same M8 Bolt, (**b**) calculated FRF, $H_{y2s.F2s}$, of the new assembly using updated joint properties

Table 57.3 Joint parameters of the M6 × 30 bolted connection

	k_{Fy} (N/m)	$k_{F\theta}$ (N/rad)	$k_{M\theta}$ (N.m/rad)	c_{Fy} (N.s/m)	$c_{F\theta}$ (N.s/rad)	$C_{L\theta}$ (N.m.s/rad)
Initial estimates	$2.06*10^6$	$7.40*10^4$	$2.9*10^3$	80.4	2.52	0.139
Updated	$2.27*10^6$	$3.89*10^4$	$3.7*10^3$	75.7	0.94	0.164

### 57.3.3 Experimental Study III: Beams Connected with M6 × 30 Hexagonal Bolt

In this experimental study, first the dynamic properties of the bolted joint using M6 × 30 mm hexagon head bolt are determined. With the identified joint parameters, the receptances of the same beams coupled with a multiple connection are calculated and compared with the measured ones.

The joint stiffness and damping values identified and updated by using the approach proposed in this study are given in Table 57.3. For initial estimates, identified results at the second mode for rotational parameters, at the third mode for translational and cross-coupling parameters are employed. By using the updated joint parameters, receptances of the assembled system are regenerated and they are compared with the measured receptances in Fig. 57.14. It can be seen from the comparison that the receptances regenerated by using the updated joint parameters perfectly match with the measured FRFs.

Finally, two M6 bolts are used to connect the same substructures, and the receptance of the new system is predicted by using the identified joint parameters and considering that there are two such joints. Comparison of the predicted FRF with the measured one shows a perfect match (Fig. 57.15), indicating that the approach proposed in this study provides a good dynamic model for a bolted joint.

In Fig. 57.16 the receptances of the coupled structure with one and two bolts, as well as with rigid connection are given. It can be seen that bolted joint adds some flexibility to the assembly, and as the number of bolts in the connection increase, assembly becomes more rigid, as expected.

Fig. 57.14 Regenerated FRF, $H_{y2s,F2s}$, of the coupled structure using updated joint properties
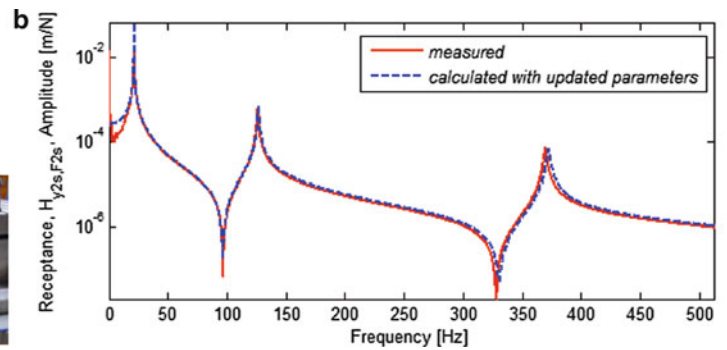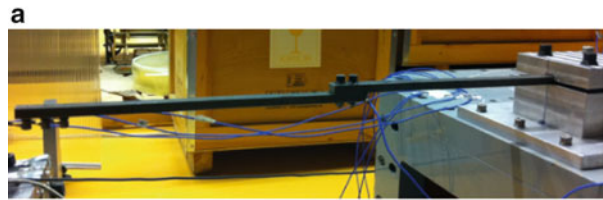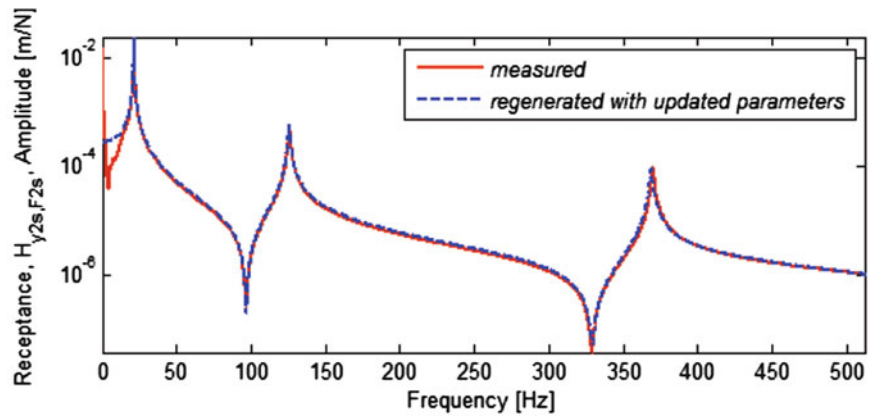
Fig. 57.15 Connection with two bolts, and calculated FRF ($H_{y2s,F2s}$) of the coupled structure using updated joint properties compared with measured one


Fig. 57.16 FRFs of the coupled structure with single bolt, two bolts and rigid connection
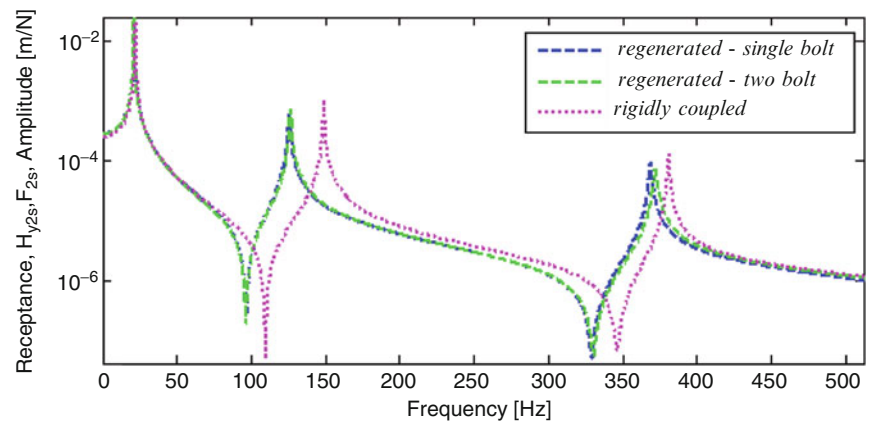
57.3.4 Effect of Bolts Size on Dynamic Properties of the Bolted Joint

The comparison of the identified stiffness and damping properties of the joints obtained by using M10, M8 and M6 bolts in this study is given in Fig. 57.17. The figure gives the identified values at each frequency, from which average values are calculated. The updated values found using these average values as initial estimates are presented in Table 57.4.

From the results obtained with the steel beams it can be concluded that as the bolt diameter is decreased stiffness parameters are increased (Table 57.4). However, a more detailed study is required to generalize this observation.
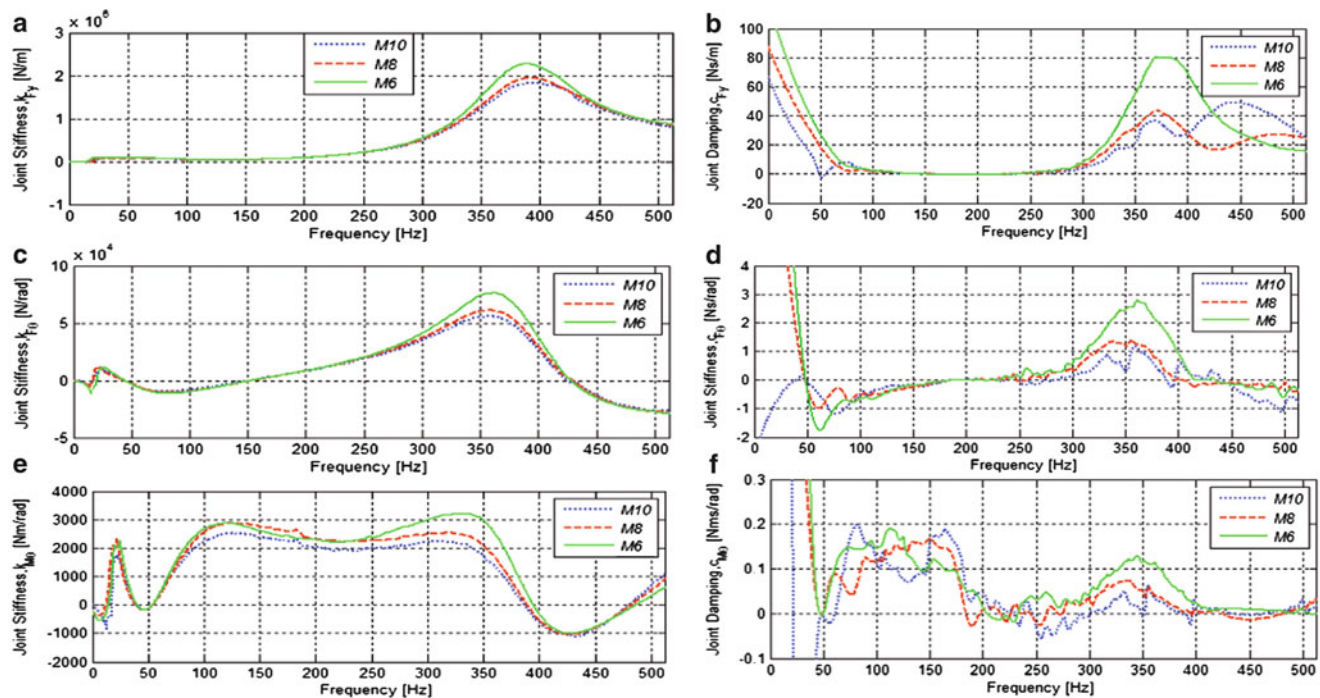
Fig. 57.17 Identified joint stiffness and joint damping values (**a**) translational joint stiffness, (**b**) cross-coupling joint stiffness, (**c**) rotational joint stiffness, (**d**) translational joint damping, (**e**) cross-coupling joint damping, (**f**) rotational joint damping

Table 57.4 Comparison of the identified joint parameters (updated values) for joints with different sizes of bolts

	k_{Fy} (N/m)	$k_{F\theta}$ (N/rad)	$k_{M\theta}$ (N.m/rad)	c_{Fy} (N.s/m)	$c_{F\theta}$ (N.s/rad)	$c_{M\theta}$ (N.m.s/rad)
M10	$2.02*10^6$	$2.47*10^4$	$2.8*10^3$	34.4	0.635	0.077
M8	$2.14*10^6$	$2.66*10^4$	$3.2*10^3$	41.2	0.845	0.119
M6	$2.27*10^6$	$3.89*10^4$	$3.7*10^3$	75.7	0.946	0.164

57.4 Discussions and Conclusions

Substructure decoupling method using measured FRFs is employed to identify dynamic properties of a structural joint. In the approach proposed, FRFs of two substructures, as well as of the coupled structure connected with bolts are measured, although it is possible to use analytically calculated FRFs for the substructures. The joint properties expressed in terms of rotational and translational stiffness and damping elements are identified by using FRF based substructure decoupling equations which were presented in a recent paper of the authors [11]. Three equations are presented for joint identification, each using a different set of FRFs but yielding the same joint properties. If we could have the exact FRF matrices for substructures and coupled structure at any frequency, any of the joint identification equations would give exactly the same and correct result at any frequency. However, due to using different sets of FRFs in each equation and due to having different measurement noise levels in each type of FRF, it is expected to have different performance from each equation. As it was mentioned in the earlier work [11], the most accurate results are obtained with Eq. (57.1a). However, from the experimental applicability point of view, among the decoupling equations the most practical one is Eq. (57.1d).

In order to make the identification more practical for real applications, rather than using RDOF related FRFs of the coupled structure it is suggested to measure and use only TDOF related ones. In the experimental applications given in this paper only one translational FRF at the tip point of the coupled structure is used in the decoupling equation, eliminating the need for estimating RDOF related FRFs from TDOF related FRFs.

The major improvement is obtained from the updating of joint parameters with an optimization algorithm, using the identified joint parameters as initial estimates. In the previous work of the authors, joint parameters are calculated by taking the average of the identification results at frequencies that belong to the mode which is most sensitive to these parameters. However, in experimental studies it is observed that the joint properties are changing with frequency due to the measurement errors at different stages and also due to the numerical errors associated with matrix inversion, and the best frequency range

to determine the joint properties may not always be so obvious. It is experimentally demonstrated that using the optimization algorithm, the joint properties can be successfully updated so that regenerated FRFs using the joint model obtained match with the experimentally measured ones at all frequencies. Three experimental case studies are presented to verify the method suggested in this work and to illustrate the accuracy and applicability of the method in real life applications. In the first case study, by using the identified bolted joint parameters the FRFs of the coupled structure are calculated at a point which is not used in the identification of joint properties and these values are found to be perfectly matching with the measured FRFs. In the second experimental case study, the identified joint parameters are used in calculating the FRFs of a new assembly constructed with the same bolt but with a beam longer than the one used in identification. The predicted FRFs are again found to be in very good agreement with experimentally measured ones. In the last experimental case study, the joint obtained with one bolt is identified and the identified joint parameters are used to predict the FRFs of the same assembly but connected with two bolts. The predicted FRFs are compared with experimentally measured ones and once again a very good match is observed. From these experimental studies it is concluded that bolted joint identification approach proposed in this study is very successful, at least for modeling bolted beam joints.

References

1. Ren Y, Beards CF (1998) Identification of effective linear joints using coupling and joint identification techniques. J Vib Acoust 120:331–338
2. Tsai JS, Chou YF (1988) The identification of dynamics characteristics of a single bolt joint. J Sound Vib 125(3):487–502
3. Wang JH, Liou CM (1991) Experimental identification of mechanical joint parameters. J Vib Acoust 113:28–36
4. Hwang HY (1998) Identification techniques of structure connection parameters using frequency response functions. J Sound Vib 212(3): 469–79
5. Yang KT, Park YS (1993) Joint structural parameter identification using a subset of frequency response function measurements. Mech Syst Signal Process 7:509–30
6. Ren Y, Beards CF (1995) Identification of joint properties of a structure using FRF data. J Sound Vib 186(4):567–587
7. Celic D, Boltezar M (2008) Identification of the dynamic properties of joints using frequency–response functions. J Sound Vib 317:158–174
8. Maia NMM, Silva JMM, Ribeiro AMR, Silva PLCGC (1998) On the dynamic characterization of joints using uncoupling techniques. In: Proceedings of the 16th international modal analysis conference, Santa Barbara, pp 1132–1138
9. Yang T, Fan SH, Lin CS (2003) Joint stiffness identification using FRF measurements. Comput Struct 81:2549–2556
10. Özşahin O, Ertürk A, Özgüven HN, Budak E (2009) A closed-form approach for identification of dynamical contact parameters in spindle-holder-tool assemblies. Int J Mach Tools Manuf 49:25–35
11. Tol Ş, Özgüven HN (2012) Dynamic characterization of structural joints using FRF decoupling. In: Topics in modal analysis I, volume 5. Conference proceedings of the society for experimental mechanics series, vol 30. Springer New York pp 435–446
12. Duarte MLM, Ewins DJ (2000) Rotational degrees of freedom for structural coupling analysis via finite-difference technique with residual compensation. Mech Syst Signal Process 14(2):205–227
13. Young MS, Tiwari M, Singh R (2007) Identification of joint stiffness matrix using a decomposition technique. In: Proceedings of 25th international modal analysis conference, Orlando